Energy xxx (xxxx) xxx

Contents lists available at ScienceDirect

Energy

journal homepage: www.elsevier.com/locate/energy

CO_2 capture cost saving through waste heat recovery using transport membrane condenser in different solvent-based carbon capture processes

Qiufang Cui [a, b, 1], Te Tu [a, b, 1], Long Ji [a, b], Shuiping Yan [a, b, *]

[a] College of Engineering, Huazhong Agricultural University, No.1, Shizishan Street, Hongshan District, Wuhan, 430070, PR China
[b] Key Laboratory of Agricultural Equipment in Mid-lower Yangtze River, Ministry of Agriculture and Rural Affairs, Wuhan, 430070, PR China

ARTICLE INFO

Article history:
Received 21 August 2020
Received in revised form
7 October 2020
Accepted 1 November 2020
Available online xxx

Keywords:
CO_2 desorption
Regeneration
Reboiler duty
Energy saving
CO_2 capture

ABSTRACT

In this study, the waste heat from the hot stripping gas was recovered by adopting the transport membrane condenser (TMC) in the monoethanolamine (MEA)-, diethanolamine (DEA)-, piperazine (PZ)- and potassium glycinate (PG)-based rich-split modified carbon capture processes. A 220-h test showed that TMC can exhibit a good stability on the waste heat recovery performance. The PZ-based TMC-modified rich-split process (i.e., PZ-case) achieved a highest waste heat recovery performance, followed by the PG-case, MEA-case and DEA-case. A strong linear relationship between the heat and water fluxes was observed during the waste heat recovery. Three scenarios were considered for comparing the CO_2 capture cost savings of 4 cases. When the TMC area was fixed meaning the same additional investment of rich-split modification, PZ-case gained the highest CO_2 capture cost saving ($6.40/t-$CO_2$), followed by PG-, MEA- and DEA-case. When a fixed waste heat recovery performance of 600 kJ/kg-CO_2 was required for obtaining the same revenue after rich-split modification, PZ- and PG-case obtained the same CO_2 capture cost saving of $4.22/t-$CO_2$. Moreover, when the reboiler duty reduction potential was aimed at 15%, PG-case achieved the maximum CO_2 capture cost saving ($4.56/t-$CO_2$).

1. Introduction

CO_2 capture and storage (CCS) is always regarded as a mainly potential method to control CO_2 emissions for preventing the anthropogenic climate change [1–3]. Due to the technical superiority and successful commercial applications, CO_2 chemical absorption method is considered as one of the most mature CO_2 capture technologies [3,4]. However, a high CO_2 regeneration energy consumption is still one of big issues for CO_2 chemical absorption process [2,5].

In the rich-split (RS) modified CO_2 chemical absorption process, a small portion of cold CO_2-rich solvent is directly split from the main rich solvent stream into the top of CO_2 stripper to recover the latent heat contained by the stripping gas (i.e., the water vapor balanced by CO_2) [5–7]. This method is always called the conventional RS carbon capture process as shown in Fig. 1. Furthermore, a metal heat exchanger is provided to act as the heat exchange medium between the bypassed cold rich solvent and the hot stripping gas for enhancing the waste heat recovery performance (HRP) [7]. These modifications generally lead to a low reboiler duty saving because of the limited heat transfer efficiency between the split cold rich solvent and hot stripping gas.

The transport membrane condenser (TMC) has been proposed by the Gas Technology Institute (GTI) to successfully recover water and waste heat from the wet flue gases by adopting the nanoporous hydrophilic ceramic membrane [8,9]. When a 2–50 nm pore-sized hydrophilic ceramic membrane is adopted in the water recovery process, a so-called capillary condensation mechanism always occurs and dominates the water transfer [10–13]. During water recovery, as the partial pressure of water vapor in the gas streams is generally higher than the capillary condensation pressure [12], the water vapor is quickly condensed in the nanoscale membrane pores through the capillary condensation mechanism to form a curved meniscus. Driven by the combined actions between the capillary force gradient and transmembrane pressure difference of water vapor, the condensate at the gas-meniscus interface can be

* Corresponding author. College of Engineering, Huazhong Agricultural University, No.1, Shizishan Street, Hongshan District, Wuhan, 430070, PR China.
E-mail address: yanshp@mail.hzau.edu.cn (S. Yan).
[1] These authors contributed equally to this work.

https://doi.org/10.1016/j.energy.2020.119225
0360-5442/

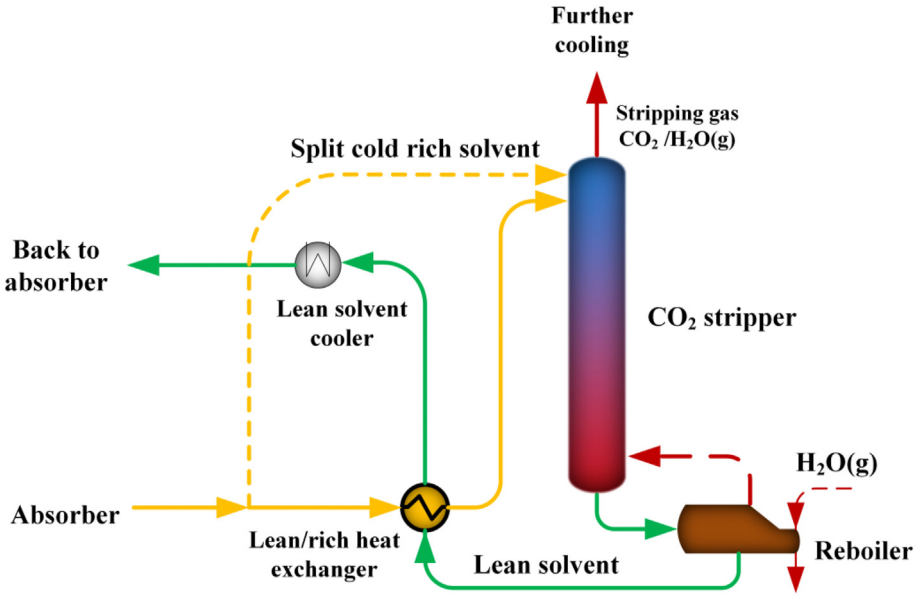

Fig. 1. Schematic diagram of conventional rich-split (RS) modified carbon capture process (only showing the regeneration stage herein).

continually sucked into the pores and then transferred across the membrane through the viscous surface flow [12,14]. Compared to the multilayer diffusion, the capillary condensation mechanism contributes to a higher condensable gas transfer flux across the membrane [12]. Additionally, the heat transfer related to the mass transfer occurs, suggesting a high heat transfer performance in the TMC [15]. Clearly, compared to the impermeable metal heat exchanger without gas-liquid mass transfer, the TMC can achieve a high HRP value mainly caused by the coupled heat and mass transfer across the membrane [8,16,17]. Moreover, TMC exhibits an excellent potential of industrial applications due to its unique advantages like the superior chemical durability and thermal stability, high specific surface area and easy cleaning [18]. In recent years, TMC has been extensively investigated for water and/or waste heat recovery from flue gases in the bench-scale test rigs [10,16,19,20] or pilot plants [9,21,22].

Obviously, TMC is promising to replace the normal impermeable metal heat exchanger in the conventional RS carbon capture process. Then the conventional RS process can be retrofitted to a so-called TMC-modified RS carbon capture process. Previously, TMC has been theoretically and experimentally confirmed to increase the HRP value from the stripping gas [14,23–25]. However, almost all the studies concerning the effects of membrane pore size [14], membrane materials [24,26] and module arrangements [25] were just grounded on the monoethanolamine (MEA)-based RS carbon capture process. Additionally, the adaptability of TMC has not been discussed yet for the RS carbon capture processes using different solvents. Due to the various solvent properties like the specific heat capacity and rich solvent flow rates related to the solvent concentration and CO_2 cyclic capacity, different solvents may generate various HRP values even at the same stripping gas conditions and TMC area. So the experimental HRP data originated from the MEA-based case cannot be embedded directly into other TMC-modified RS processes using different solvents. Correspondingly, the reduction potentials of CO_2 capture cost induced by the waste heat recovery is definitely different between MEA- and other solvents-based RS processes adopting TMC. Clearly, there are some knowledge gaps with respect to the difference of waste heat recovery performance and CO_2 capture cost saving among different solvents-based rich-split carbon capture processes. Thus, it is of importance to explore the application prospects of TMC-modified RS carbon capture processes using different solvents in terms of HRP values and then the corresponding carbon capture cost savings.

In this study, four typical absorbents including MEA, diethanolamine (DEA), piperazine (PZ) and potassium glycinate (PG) were experimentally investigated in a TMC-modified RS carbon capture process. MEA and DEA are the commonly used absorbents [27]. In recent years, PZ has been extensively investigated to replace MEA due to its better resistance to oxidation, low volatility and fast CO_2 reaction rate [28]. Labelled as the environmentally-friendly absorbents, amino acid salts have also been tested as the alternatives to separate CO_2 from CO_2-rich gas streams [27]. So a typical amino acid salt, PG was chosen herein as well. The stability of TMC-modified RS process was firstly tested by a 220-h long-term operation. Then the HRP value from the mimic stripping gas by TMC was tested and compared under the changed operating conditions. According to the erected empirical correlations between the heat flux and mass flux, the development of TMC in the further work was proposed. Finally, the techno-economic analysis of TMC-modified RS processes using these four solvents was conducted to assess the CO_2 capture cost savings resulted from the waste heat recovery at three different scenarios.

2. Materials and methods

2.1. Materials

2.1.1. Ceramic membrane tube

A 4-nm pore-sized nanoporous hydrophilic ceramic membrane with 8-mm I.D., 12-mm O.D. and 200-mm length was capsulated into a 304 stainless-steel shell with 15-mm I.D. and 19-mm O.D. as a single TMC in this study, which can be seen in Fig. 2. Two TMCs were serially arranged to act as the heat exchanger between the stripping gas and bypassed rich solvent. So, the total heat exchange area is about 0.01 m^2. The ceramic membrane tube whose separation layer is coated on the inner side, and the stainless-steel shell were both provided by Nanjing Aiyuqi Membrane Science and Technology Co., Ltd., China. Properties of the single ceramic membrane tube and single shell are listed in Table 1. The sessile drop method was performed to test the water contact angle of ceramic

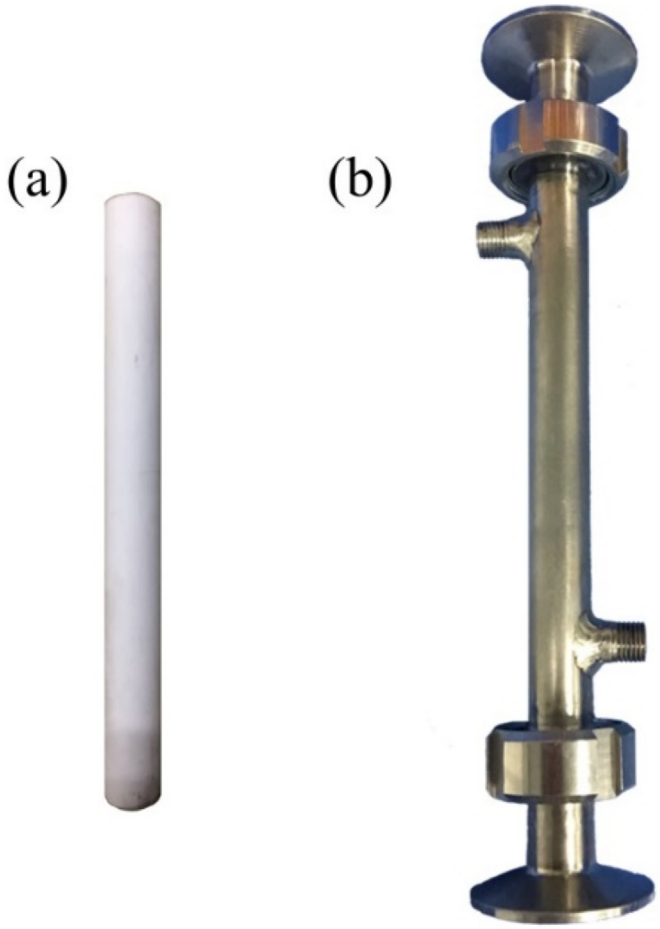

Fig. 2. Ceramic membrane tube (a) and stainless-steel shell (b) used in this study.

Table 1
Properties of a single ceramic membrane tube and stainless shell in this study.

Item	Parameter	Value
Single ceramic membrane tube	Length (mm)	200
	Membrane area (m^2)	0.005
	Average pore size (nm)	4
	O.D./I.D. (mm)	12/8
	Material	Al_2O_3, ZrO_2, TiO_2
	Porosity (%)	23.1
	Water contact angle (°)	59.5
Single shell	Effective length (mm)	200
	O.D./I.D. (mm)	19/15
	Number of tubes	1

membrane in a contact angle meter (OCA15EC, Dataphysics Instruments, Filderstadt, Germany).

2.1.2. Absorbents

MEA (Analytical Reagent (AR), purity > 99%), DEA (AR, purity > 99%), PZ (AR, purity > 99%) and PG with different concentrations were adopted to form the CO_2-rich solvents in this study. Aqueous MEA, DEA and PZ solutions were prepared by dissolving the pure MEA and DEA liquids and PZ solid into the ultra-purity (UP) water to form the desired mass concentrations. PG was prepared by the neutralization of glycine (AR, purity > 99%) with the equal molar KOH (AR, purity > 85%) in the UP water. Then pure CO_2 (purity >99.9 mol.%) from WISCO Oxygen Co., Ltd. (China) was introduced into these solutions to reach the desired CO_2 loadings.

Table 2
Information of absorbents used in this study.

Solvent	Concentration (wt.%)	CO_2 loading (mol/mol)	Net cyclic CO_2 capacity (mol/mol)	Ref.
MEA	10–40	0.45	0.25	[14]
DEA	15–45	0.5	0.4	[28]
PZ	2–8	0.8	0.5	[29,30]
PG	10–40	0.5	0.3	[31]

The information on absorbents is listed in Table 2. Due to the limited water solubility, a relatively low PZ concentration was adopted in this study.

2.2. Experimental setup and procedure

Fig. 3 shows the experimental apparatus and procedure in this study. In the gas side, the CO_2 gas from the gas cylinder and UP water with the precisely controlled mass flow rates were introduced simultaneously into a spiral coil heater immersed in a thermostat oil heater, in which water was totally evaporated to water vapor having a same temperature with CO_2. The mixture of CO_2 and water vapor was used to mimic the hot stripping gas in the real CO_2 capture process. The mimicked hot stripping gas went into the lumen of TMC placed horizontally. After reaching the desired temperature by heating, CO_2-rich solvent was directly pumped from the solvent tank into the shell of TMC for recovering the waste heat and water vapor from the stripping gas. In the TMC, the liquid was flowed countercurrently with the stripping gas. By controlling the mass flow rate of rich solvent, the split fraction of cold rich solvent (η) bypassed from the main rich solvent stream into the TMC in the RS carbon capture process was simulated. The η value can be calculated by the mass flow rate ratio of cold rich solvent flowed in the TMC to the total rich solvent discharged from CO_2 absorber [7,14].

After heat exchanging, the outlet stripping gas with a low temperature and water vapor content was condensed in a −2 °C cold trap to further separate water vapor from CO_2 so as to assess the mass transfer of water across the membrane. Notably, CO_2 mass transfer from the gas side to the solvent side across membrane was ignored because of a low water solubility of CO_2 in the capillary condensate occurred in the nanoscale ceramic membrane pores [10,32]. The outlet liquid pipeline was set at a position slightly higher than the TMC in order to obtain a completely liquid-filled shell. Four thermometers were installed in the inlet and outlet of gas mixture and liquid sides to calculate the recovered heat flux. In order to reduce the heat loss, the TMC and all gas and liquid pipelines were covered with the 10-cm thick quartz cotton.

2.3. Determination of heat and water recovery performance

There are so many indexes available to represent the waste heat and water recovery performance of TMC [21]. In this study, the CO_2 regeneration heat saving (Q in kJ/kg-CO_2) and water flux (J in kg/(m^2 h)) were used to evaluate the waste heat and water recovery performance in the TMC, respectively.

The total recovered heat in the TMC generally consists of two parts: the heat related to the mass transfer across the membrane and the heat by membrane conduction [15]. Thus, the HRP value of TMC can be calculated using Equation (1). This recovered waste heat can be transferred by the bypassed cold CO_2-rich solvent into the stripper for reducing the CO_2 regeneration heat consumption, which is usually considered as the reboiler duty saving at a suitable split fraction.

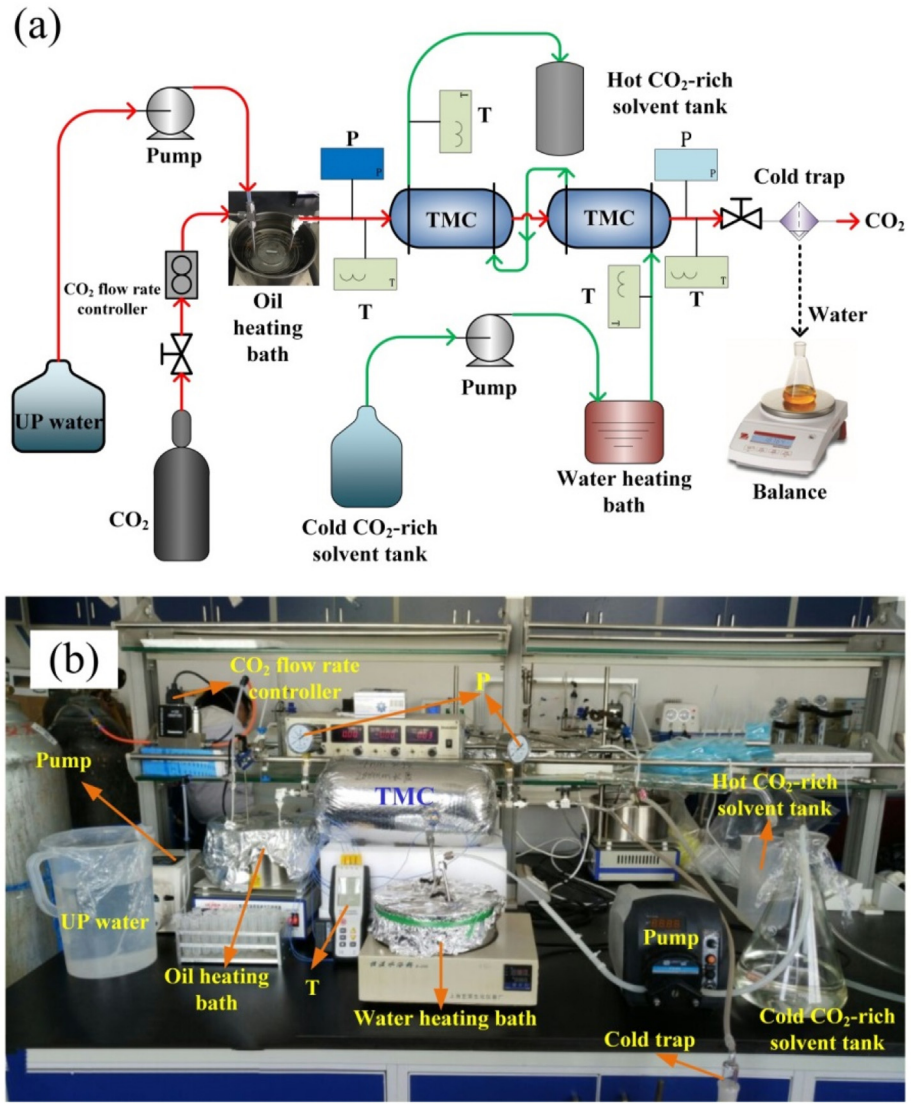

Fig. 3. Schematic diagram (a) and photograph (b) of the waste heat recovery experimental set-up using TMC in this study.

$$Q = \frac{m_{sol}^{out} \cdot h_{sol}(T) - m_{sol}^{in} \cdot h_{sol}(T)}{m_{CO_2}} = 22.4 \cdot \frac{c\overline{m_{sol}}\Delta T + J \cdot A \cdot h_w(T)}{44 \cdot V_{CO_2}} \quad (1)$$

where Q is the total recovered heat, kJ/kg-CO_2; m_{sol}^{in} and m_{sol}^{out} are the inlet and outlet mass flow rates of bypassed cold rich solvent in kg/h, respectively; $h_{sol}(T)$ is the enthalpy of rich solvent at the temperature T, kJ/kg; m_{CO_2} and V_{CO_2} is the inlet CO_2 mass flow rate in kg/h and volumetric flow rate in Nm^3/h, respectively; c is the averaged specific heat capacity of rich solvent, kJ/(kg K); $\overline{m_{sol}}$ is the average mass flow rate of bypassed rich solvent, kg/h; ΔT is the temperature difference between inlet and outlet rich solvent, °C; $h_w(T)$ is the enthalpy of water at the temperature T, kJ/kg; A is the total membrane area, m^2; J is the total water/water vapor flow rate recovered across the membrane in kg/(m^2 h).

The heat flux per m^2 of membrane area (q in MJ/(m^2 h)) is also adopted, which can be determined as follows:

$$q = \frac{c\overline{m_{sol}}\Delta T + J \cdot A \cdot h_w(T)}{1000 \cdot A} \quad (2)$$

The water flux (J) is defined by the difference of water vapor mass flow rate between the inlet and outlet stripping gas per unit of membrane area:

$$J = \frac{m_v^{in} - m_w^{out} - \frac{44 \cdot \phi \cdot V_{CO_2}}{22.4 \cdot 1000}}{A} \quad (3)$$

where m_v^{in} is the inlet water vapor mass flow rate, kg/h; m_w^{out} is the water mass flow rate obtained from the balance, kg/h; ϕ is the absolute humidity of water vapor saturated CO_2 at −2 °C, which equals to about 2.1437 g/kg-CO_2.

The uncertainty analysis was made using the same methodology in our previous study [25]. The relative uncertainties of Q, q and J are about 0.7%, 0.3% and 3.1%, respectively.

3. Results and discussion

3.1. Long-term operating stability of waste heat recovery system using TMC

A long-term operation was carried out in order to preferably

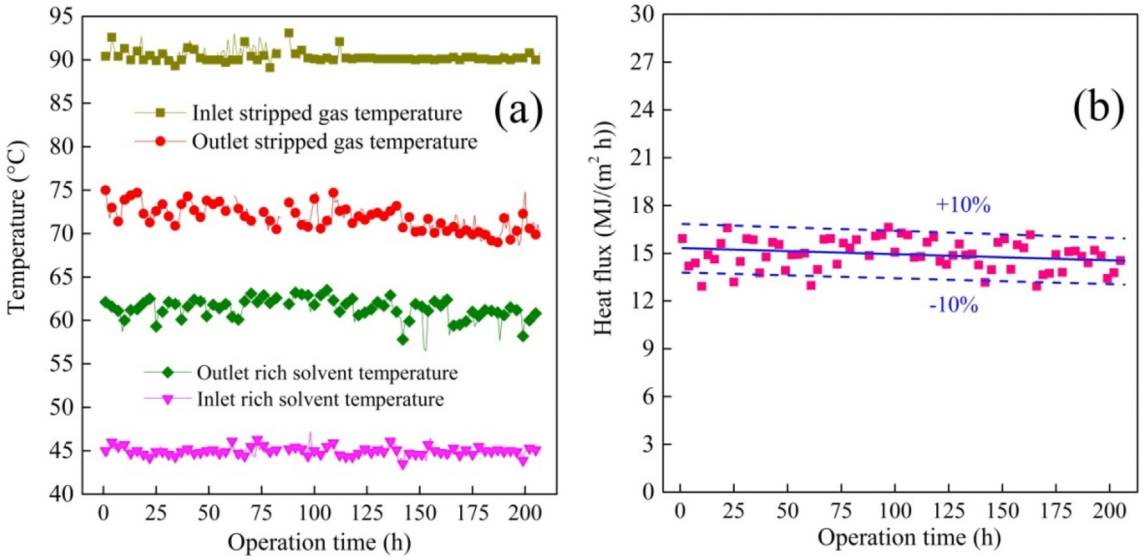

Fig. 4. Inlet and outlet temperatures of stripping gas and rich MEA solvent (a) and waste heat recovery performance (b) during a 220-h long-term operation (Experimental conditions: MEA concentration (W) = 30 wt%, CO_2 loading (α_{Tot}) = 0.45 mol/mol, inlet cold rich solvent temperature (T_{sol}^{in}) = 45 ± 5 °C, inlet rich solvent flow rate in TMC (V_{sol}) = 1.8 L/h, inlet stripping gas temperature (T_{gas}^{in}) = 90 ± 5 °C, inlet stripping gas flow rate (V_g) = 0.36 Nm^3/h, molar ratio of water vapor to CO_2 (γ) in the stripping gas = 1:1).

analyze the economy of TMC-modified RS carbon capture process. In this section, MEA was chosen. The test apparatus was running totally for 220-h and the data were recorded every hour as shown in Fig. 4. The stability of waste heat recovery system using TMC in the long-term operation can be exhibited directly by the gas and liquid temperature variations (Fig. 4a) and heat recovery performance (Fig. 4b).

Generally, the ceramic membrane is made from alumina, zirconia, titanium dioxide sintered at a high temperature (~1200 °C), which has a high mechanical strength, thermal and chemical stability. So at the experimental conditions with a relatively low gas temperature (~90 °C) and pressure (~30 kPa), the ceramic membrane can undergo these thermal and pressure attacks in a long-term operation without affecting the morphologies of its separation layer and substrate [33]. Additionally, the ceramic membrane has a relatively high hydrophilicity confirmed by its low water contact angle (59.5° as shown in Table 1), implying a low fouling problem in the heat and water recovery process because a hydrophilic surface does not promote the adhesion of the fouling layer [34,35]. As mentioned above, these advantages imply that the TMC should have a good fouling-resistance and then a good stability in the waste heat recovery process. As shown in Fig. 4a, all the inlet and outlet temperatures of the stripping gas and rich MEA solvent are nearly constant during a 220-h operation, implying a good stability of TMC on the heat recovery performance. Moreover as shown in Fig. 4b, all the heat fluxes during the 220-h operation time fall within ±10% deviation, indicating a stable waste heat recovery performance. It can be concluded that TMC is a promising to retrofit the conventional RS carbon capture process for improving the waste heat recovery performance from the stripping gas.

3.2. Waste heat recovery performance in different solvent-based TMC-modified RS carbon capture processes using the same TMC

Fig. 5 exhibits the effects of solvent concentration (W) on the HRP values in kJ/kg-CO_2 and recovered water fluxes. Notably, only these PZ solutions with 2−8% concentrations were experimented because of its easy precipitability at a high concentration [3]. Obviously, all the investigated rich solvents can successfully recover the waste heat from the stripping gas with the same conditions by a same TMC. Additionally, increasing the rich solvent concentration is detrimental to heat and water recovery, which is mainly ascribed to an increase of boundary layer thickness in the rich solvent side and a decline of specific heat capacity of rich solvent at a high solvent concentration [36−38]. Notably as shown in Fig. 5, even at the same stripping gas conditions meaning the equalized gas enthalpy, different rich solvents straightforwardly cause diverse HRP values using a same TMC. For example, in the ranges of concentration investigated, PZ case can obtain the highest HRP values at a relatively low concentration. Comparatively, DEA case achieves the lowest HRP values at a high concentration. It is reasonable that the TMC size may be smallest for PZ case than other solvent-based processes if a same HRP value is desired, showing a lowest investment for the TMC modification. The difference of HRP values among different solvents may result from the various specific heat capacities of rich solvents and different rich solvent mass flow rates in the TMC at a fixed split fraction.

In the real RS process, various mass flow rates of solvent are desired for different solvents because of the diverse solvent concentrations and net CO_2 cyclic capacities (Table 2). It means that the mass flow rates of cold rich solvent flowed in the TMC are different. So, it may be reasonable for comparing the HRP value of different solvent cases using the TMC at a fixed split fraction (η). The experimental η value can be easily assessed using the real bypassed rich mass flow rate in the TMC and total rich mass flow rate in the carbon capture process, which can be found in Table 3. The total rich mass flow rate can be figured out using the solvent concentration, regenerated CO_2 flow rate from the stripper, CO_2 loading of rich solvent and net cyclic CO_2 capacity [14]. Generally, the split fraction should be less than 0.3 for no increase in the reboiler duty [5]. Especially for MEA case, the recommended split fraction is less than 0.25 [14]. Additionally, when the split fraction is less than the critical value, an increase in split fraction can result in the improvement of waste heat recovery performance and then the decrease of CO_2 regeneration heat consumption [5,14]. Thus, a fixed η value of 0.25 was employed in this study to discuss the effects of operating conditions except the change of bypassed rich solvent and stripping gas flow rate.

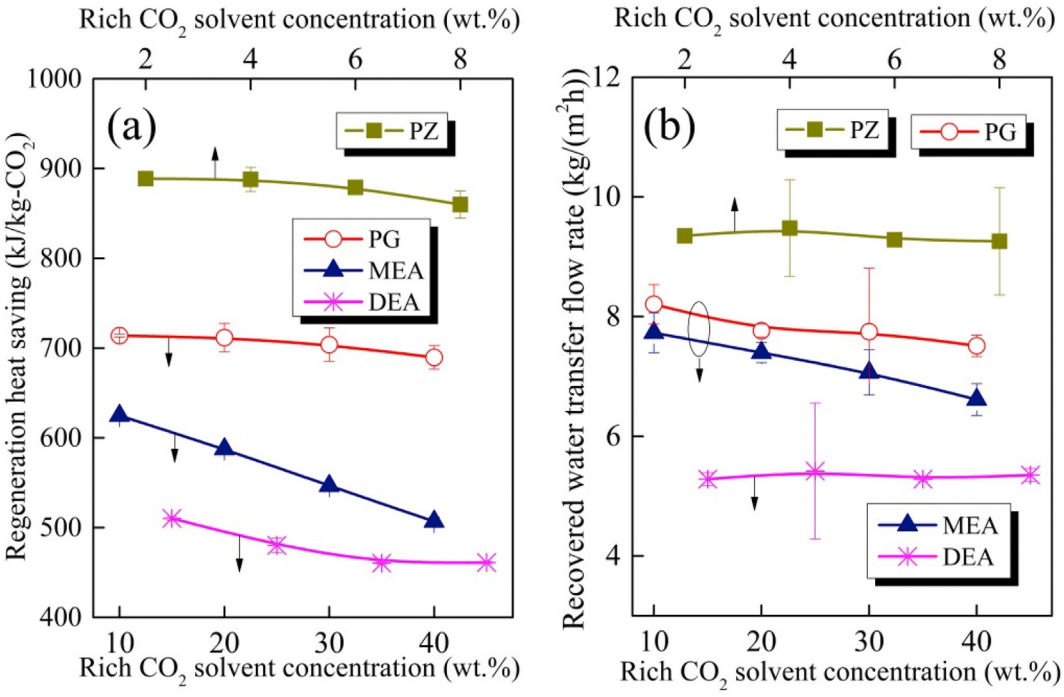

Fig. 5. Comparisons of waste heat recovery (a) and water recovery (b) performance among different solvents varied with the solvent concentration W (Experimental condition: $(T_{sol}^{in}) = 45 \pm 0.5$ °C, a fixed split fraction at about 0.25 for all the solvents (η=0.25), i.e., $(V_{sol}^{MEA}) = 1.8$ L/h, $(V_{sol}^{DEA}) = 1.44$ L/h, $(V_{sol}^{DEA}) = 2.16$ L/h, $(V_{sol}^{PZ}) = 4.5$ L/h; $(\alpha_{Tot}^{MEA}) = 0.45$ mol/mol, $(\alpha_{Tot}^{DEA}) = 0.5$ mol/mol, $(\alpha_{Tot}^{PG}) = 0.5$ mol/mol, $(\alpha_{Tot}^{PG}) = 0.8$ mol/mol; $(T_{gas}^{in}) = 90 \pm 0.5$ °C, $V_g = 0.36$ Nm^3/h, γ = 1:1, inlet stripping gas pressure (P) = 106.3 kPa).

Table 3
Experimental split fractions of rich solvents in this study.

Solvents	Bypassed cold rich solvent mass flow rate, m_{sol}^{By} (kg/h)	Calculated total flow rate of rich solvent, m_{sol}^{Tot} (kg/h)	Split fraction, η
MEA	0.9–4.5	7.2	0.12–0.63
DEA	0.7–3.6	6.5	0.11–0.56
PG	0.9–4.3	11.4	0.08–0.37
PZ	1.8–5.4	17.9	0.1–0.3

(Notes: When calculating the split fractions, the concentrations were fixed at 30 wt% for MEA, 35 wt% for DEA, 30 wt% for PG and 8 wt% for PZ, respectively.).

Unsurprisingly, a low PZ concentration leads to a high total flow rate of rich solvent as shown in Table 3. So at a fixed η value of 0.25, a high PZ solvent mass flow rate bypassed into the TMC is required, leading to a high HRP value due to the reduction of heat transfer resistance in liquid phase [14]. Similarly, a high solvent mass flow rate can reduce the resistance of water transfer from the gas side into solvent side across the membrane, resulting in a high water transfer performance as shown in Fig. 5b, and consequently more convection heat flux related to the mass transfer [15,39]. Moreover, according to Equation (1), the different specific heat capacity of solvent is another reason that causes the disparity of recovered heat flux [36,37,40].

Under other operation conditions, the HRP values for different cases are shown in Fig. 6. As shown in Fig. 6, PZ case always demonstrates a highest HRP value among all the 4 tested solvents using a same TMC. With an increase of bypassed rich solvent flow rate in the TMC as shown in Fig. 6a, the HRP value shows a similar exponential increase trend for all the cases. That is because at a high solvent mass flow rate, a high convection heat transfer coefficient on the liquid side resulted from the decrease of heat boundary layer thickness can be obtained to increase the temperature difference between the bulk stripping gas and the inner membrane surface [24], consequently bring about an increase in water vapor condensation rate [41]. Interestingly, even at a same flow rate, PZ case still achieves a highest HRP value than other 3 cases, which may be mainly ascribed to its highest specific heat capacity.

As shown in Fig. 6b, the HRP value for all the 4 cases shows a sharp drop with the increase of the inlet rich solvent temperature. These phenomena can be expected because the gas-liquid temperature difference decreases with an increase in the rich solvent temperature at a fixed gas temperature, resulting in a great decrease of heat transfer driving force and consequently a gigantic decline in the HRP value [42]. Furthermore, PZ case still shows the best HRP value at a fixed η value due to its highest mass flow rate and specific heat capacity.

Fig. 6c illustrates the negative correlations between the HRP value and the stripping gas volumetric flow rate for all the 4 cases. Increasing the gas flow rate can straightforwardly result in the growth of condensable water vapor amount in the TMC [43], causing an increase in the released water vapor condensation latent heat. However, a short gas residence time in the TMC also happens at a high gas flow rate. So the increase of gas flow rate does not stimulate a proportional increase in the total heat recovery. Therefore, the HRP value decreases. Additionally, PZ case still achieves the highest HRP value due to the same reasons as mentioned above.

Despite a great rise in the inlet stripping gas temperature at the experimental ranges from 90 °C to 110 °C, the HRP value only shows a slight change as shown in Fig. 6d. At a fixed water vapor molar fraction in the stripping gas, the enthalpy of inlet stripping gas mainly determined by the water vapor enthalpy only increases slightly but the system heat loss rises with the increase of gas temperature, which results in a low heat transfer coefficient [24,44]. So the gas temperature shows a minor effect on HRP value.

All the results showed that the TMC has a good adaptability and practicability in different solvent-based RS carbon capture

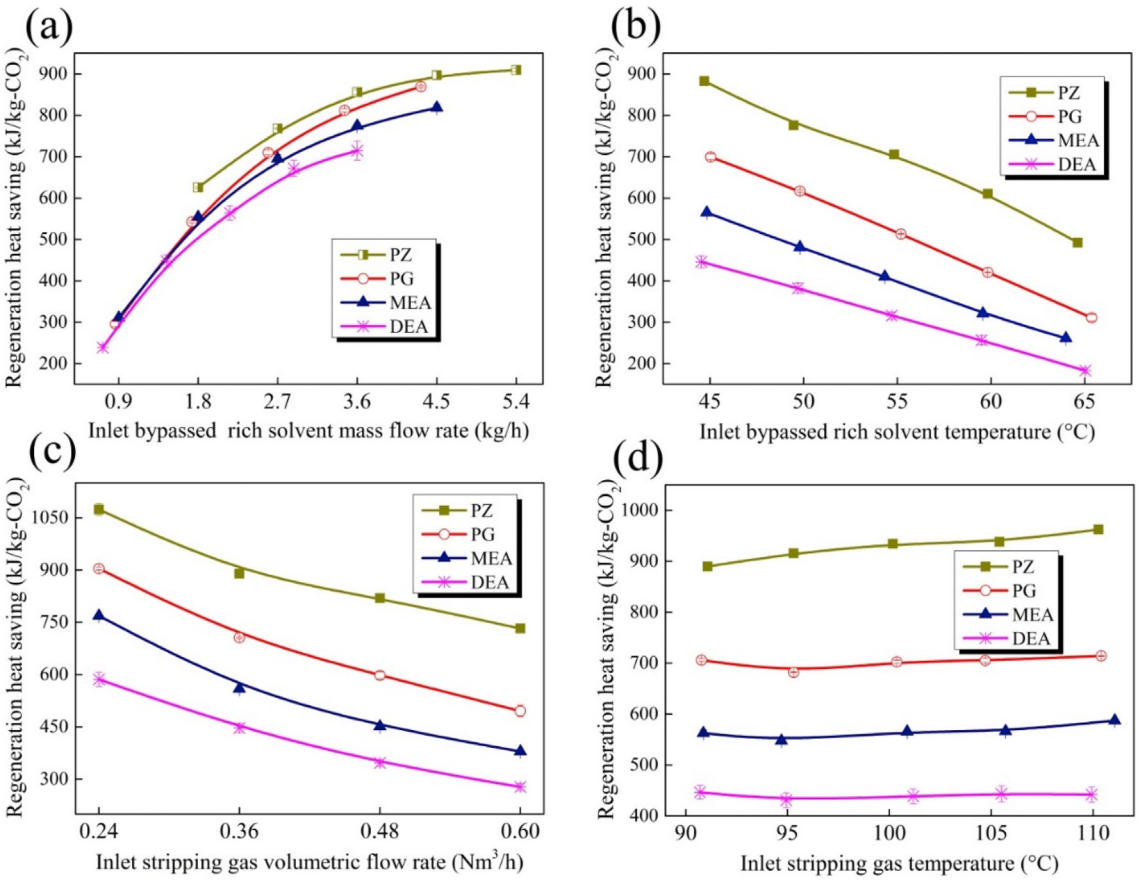

Fig. 6. Effect of the rich solvent mass flow rate (a) and temperature (b), stripping gas volumetic flow rate (c) and temperature (d) on the heat recovery performance (Q value) (Experimental conditions: W^{MEA} = 30 wt%, W^{DEA} = 35 wt%, W^{PG} = 30 wt%, W^{PZ} = 8 wt%, (α_{Tot}^{MEA}) = 0.45 mol/mol, (α_{Tot}^{DEA}) = 0.5 mol/mol, (α_{Tot}^{PG}) = 0.5 mol/mol, (α_{Tot}^{PZ}) = 0.8 mol/mol, γ = 1:1. And for (a): (T_{sol}^{in}) = 45 ± 0.5 °C, (T_{gas}^{in}) = 90 ± 0.5 °C, V_g = 0.36 Nm^3/h, P = 105.3–107.3 kPa; for (b): η = 0.25, i.e., m_{sol}^{MEA} = 1.8 kg/h, m_{sol}^{DEA} = 1.44 kg/h, m_{sol}^{PG} = 2.6 kg/h, m_{sol}^{PZ} = 4.5 kg/h, (T_{gas}^{in}) = 90 ± 0.5 °C, V_g = 0.36 Nm^3/h, P = 105.3–109.3 kPa; for (c): (T_{sol}^{in}) = 45 ± 0.5 °C, m_{sol}^{MEA} = 1.8 kg/h, m_{sol}^{DEA} = 1.44 kg/h, m_{sol}^{PG} = 2.6 kg/h, m_{sol}^{PZ} = 4.5 kg/h, (T_{gas}^{in}) = 90 ± 0.5 °C, P = 106.3 kPa; for (d): (T_{sol}^{in}) = 45 ± 0.5 °C, η = 0.25, i.e.,m_{sol}^{MEA} = 1.8 kg/h, m_{sol}^{DEA} = 1.44 kg/h, m_{sol}^{PG} = 2.6 kg/h, m_{sol}^{PZ} = 4.5 kg/h, V_g = 0.36 Nm^3/h, P = 106.3 kPa).

processes. Notably, PZ case has the highest HRP value. Such results also claim that when a fixed reduction of CO_2 regeneration heat consumption (i.e., reboiler duty saving) is desired, PZ case requests a lowest TMC area, meaning a lowest TMC investment.

3.3. Empirical correlations between heat and mass fluxes in different solvent-based TMC-modified RS carbon capture processes

During the heat exchange between the hot stripping gas and cold rich solvent in the TMC, the coupled heat and mass transfers occur, and the convection heat flux related to the mass transfer contributes to enhancing the total heat flux and consequently the HRP value [8,24]. To investigate the correlations between the heat transfer and mass transfer for different solvent-based systems, four empirical correlations are established using the water flux (J) as X-axis and heat flux (q) in MJ/(m^2 h) as Y-axis (Fig. 7). According to Fig. 7, there is a strong linear relationship between the heat flux and water flux for every solvent-based system [24]. Evidently, an increase in water flux during heat exchange in TMC leads to a great growth of HRP value, showing the necessity of developing the novel membranes featured with a high water transfer performance. For a given CO_2 regeneration process, water transfer can be enhanced by membrane modification [20]. Additionally, the novel membranes featured with a high water transfer performance should be focused in the future for further enhancing the waste heat recovery performance. Among all the 4 cases, PZ case is more sensitive to the change of water flux, followed by MEA, DEA and PG cases.

3.4. CO_2 capture cost savings for different solvent-based RS carbon capture processes through waste heat recovery by TMC

3.4.1. Methodology of economic analysis

A CO_2 chemical absorption project for treating ~8000 Nm^3/h flue gas is taken as an example. In this project, CO_2 concentration in the flue gas is ~13 vol%, and CO_2 capture efficiency is set at 90% [45]. A conventional CO_2 chemical absorption process is adopted as the baseline, and MEA, DEA, PZ and PG are separately considered as the CO_2 absorbents. So there are 4 baseline cases. After TMC modification in the RS carbon capture process, there are accordingly 4 cases named MEA-case, DEA-case, PZ-case and PG-case for investigating the potential of CO_2 capture cost saving for different absorbent processes. The fundamental data for TMC-modified rich-split process are presented in Table 4. Only the best split fractions of bypassed cold rich solvent in the TMC originated from the experiments are considered for all the 4 cases.

When the TMC-based RS modification is implemented, only the TMC, pipelines, liquid pumps and some valves are added into the conventional CO_2 regeneration stage as shown in Fig. 1. These additional investments and the corresponding operation and maintenance (O&M) costs directly lead to the increase of CO_2 capture cost. However, after RS modification, the waste heat carried by the stripping gas is recovered, causing the reduction of reboiler

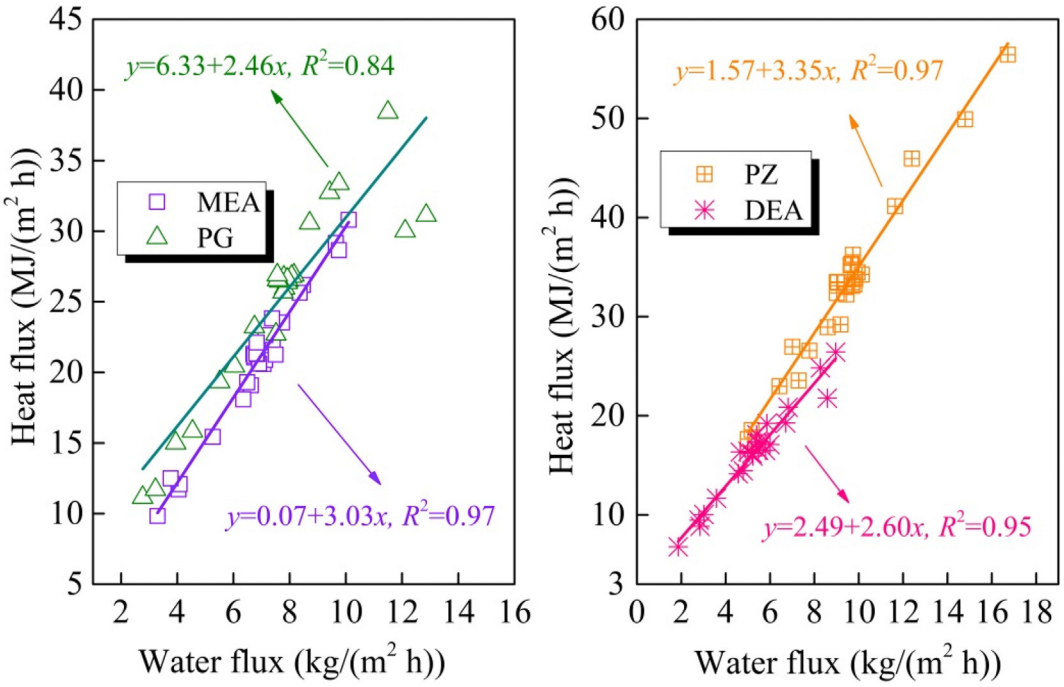

Fig. 7. Relationship between water flux and heat flux during waste heat recovery for different solvent-based TMC-modified RS carbon capture processes.

Table 4
Basic data for TMC-modified RS carbon capture process.

Items	Value	Ref.
γ (n_{H_2O}:n_{CO_2})	1:1	
η ($m_{sol}^{By}/m_{sol}^{Tot}$) (−)	0.25	
Steam price ($/GJ)	8.4	[46]
Electricity price ($/kWh)	0.09	[47]
Membrane price ($/m^2)	378.2	[21]
Stainless-steel price ($/t)	2941	[21]
Consumption of stainless steel per unit membrane area (kg/m^2)	25.3	[21]
Membrane lifetime (year)	5	
Year depreciation rate (%)	4	
Annual operating time (h)	5500	
Design life (year)	25	

(Note: 1 $ = 7.14 ¥ in the second quarter of 2020 in China).

duty and consequently the drop of steam cost in the reboiler. The decline of steam cost during CO_2 regeneration results in the decrease of O&M cost and then drop of CO_2 capture cost. If the potential revenue from the steam saving (POREV) is higher than the expenditure ascribed to the additional investment and O&M costs (EXP), TMC-based RS modification is reasonable for the carbon capture process. The POREV value in $/t-$CO_2$ can be calculated by multiplying the steam price by the steam saving equalized to the recovered waste heat (i.e., HRP value in the experiments). The EXP value includes the yearly depreciation cost of rich-split process modification, membrane replacement cost, maintenance cost and the additional electricity cost pump for driving the partial cold rich solvent into the TMC. This calculation of additional power consumption can be found elsewhere [48]. The treated flow rates of stripping gas per unit of membrane area can be calculated by the experimental results as shown in Fig. 6 and then the required membrane area can be linearly amplified in this project. So the total CO_2 capture cost saving for TMC-based RS modification can be easily assessed by the difference between POREV and EXP values.

3.4.2. Scenario 1: CO_2 capture cost savings at a fixed TMC area

In this scenario, CO_2 capture cost savings were investigated in the premise of an equalized TMC investment for all the 4 cases. However, even at a fixed TMC area, POREV values are various for the 4 cases because of their different waste heat recovery performance at a fixed TMC area as mentioned above. Thus, the CO_2 capture cost saving is mainly controlled by the POREV value. Economic evaluations of these 4 cases are listed in Table 5.

As shown in Table 5, CO_2 capture savings ranged from $2.77/t-$CO_2$ to $6.4/t-$CO_2$ can be achieved for different cases, implying that the TMC-based RS modification is profitable for carbon capture process. Notably, although PZ-case has the highest EXP value mainly caused by its highest cold rich solvent flow rate in the TMC at a fixed split fraction, it can still obtain a highest CO_2 capture cost saving, followed by PG-case, MEA-case and DEA-case. This is mainly ascribed to the highest HRP value for PZ-case. Compared to other solvent-based processes at a fixed additional investment, PZ-based carbon capture process may be more suitable for the TMC-based RS modification to acquire a lower CO_2 capture cost. Moreover, the membrane replacement cost accounts for about 36–42% of EXP value (Table 5), indicating that the development of novel membrane with a low price and long lifetime can further reduce the CO_2 capture cost.

3.4.3. Scenario 2: CO_2 capture cost savings at a fixed waste heat recovery performance

In this scenario, a fixed HRP value of 600 kJ/kg-CO_2 is considered for all four cases. Then the POREV value dominated by the HRP value is fixed and the CO_2 capture cost saving is decided by the EXP value as summarized in Table 6.

Due to the discrepancy of EXP values among four cases, the CO_2 capture savings change from $3.67/t-$CO_2$ to $4.22/t-$CO_2$ as shown in Table 6. In spite of the same HRP value, the corresponding required membrane areas are different attributed to the various heat fluxes in the TMC for different cases. Coincidentally, both PZ-case and PG-case have the same highest CO_2 capture saving of

Table 5
Economic analysis of TMC-modified RS carbon capture processes using different absorbents at a fixed TMC area.

Item	Value			
Case No.	MEA-case	DEA-case	PZ-case	PG-case
Stripping gas volumetric flow rate per unit of membrane area, $V_{\bar{A}}$ ($Nm^3/(h \cdot m^2)$)	36			
Solvent flow rate (kg/h)	37.4	30.0	93.6	53.9
Waste heat recovery performance, HRP (kJ/kg-CO_2)	559	439	889	706
Required membrane area (m^2)	52			
Additional cost of auxiliaries (valves, pipelines and pumps) ($)	14,006			
Additional cost of construction ($)	7499			
Additional yearly depreciation cost of RS modification ($/year)	1800			
Membrane replacement cost, C_M ($/year)	3933			
Additional cost of maintenance ($/year)	2801			
Power consumption cost (liquid pump), C_P ($/year)	934.3	747.4	2335.7	1121.1
Additional operation cost ($/year)	9468	9281	10,869	9655
Expenditure due to the additional investment and O&M costs, EXP ($/t-$CO_2$)	0.94	0.92	1.07	0.95
Potential revenue due to steam saving, POREV ($/t-$CO_2$)	4.70	3.69	7.47	5.93
CO_2 capture cost saving ($/t-$CO_2$)	3.76	2.77	6.40	4.98

(Notes: the construction cost is 0.2 times of the costs of auxiliaries, membrane, and stainless-steel shell [21]; CO_2 capture cost saving = POREV-EXP).

Table 6
Economic analysis of TMC-modified RS carbon capture processes with different absorbents at a fixed waste heat recovery performance.

Item	Value			
Case No.	MEA-case	DEA-case	PZ-case	PG-case
HRP value (kJ/kg-CO_2)	600	600	600	600
$V_{\bar{A}}$ ($Nm^3/(h \cdot m^2)$)	33.6	19.0	72.6	48.8
Solvent flow rate (kg/h)	37.4	30.0	93.6	53.9
Required membrane area (m^2)	55.7	98.7	25.8	38.3
Additional cost of auxiliaries (valves, pipelines and pumps) ($)	14,006			
Additional cost of construction ($)	7842	11,735	5134	6269
Additional yearly depreciation cost of RS modification ($/year)	1882	2816	1232	1505
C_M ($/year)	4214	7467	1950	2899
Additional cost of maintenance ($/year)	2801			
C_P ($/year)	934.3	747.4	2335.7	1121.1
Additional operation cost ($/year)	9831	13,832	8319	8326
EXP ($/t-$CO_2$)	0.97	1.37	0.82	0.82
POREV ($/t-$CO_2$)	5.04	5.04	5.04	5.04
CO_2 capture cost saving ($/t-$CO_2$)	4.07	3.67	4.22	4.22

$4.22/t-$CO_2$ due to the same EXP and POREV values. Compared with PG-case, PZ-case has the lower yearly depreciation and membrane replacement costs caused by the smaller membrane area requirement, while its high solvent flow rate also leads to a higher power consumption cost.

3.4.4. Scenario 3: CO_2 capture cost savings at a fixed reduction rate of reboiler duty

At a fixed reduction ratio of reboiler duty defined by the ratio of waste heat recovery to the reboiler duty of the baseline case, economic analyses of TMC-modified RS carbon capture processes using different absorbents are shown in Table 7. In this scenario, a 15% reduction rate of reboiler duty was considered.

As shown in Table 7, unlike Scenarios 1 and 2, PG-case has the highest CO_2 capture cost saving of $4.56/t-$CO_2$ than other cases in this scenario. At a fixed reboiler duty reduction rate, a different reboiler duty straightforwardly results in a diverse requirement of HRP value, and consequently a various POREV value. Obviously, PG-case has the highest POREV value among all the 4 cases because of its highest HRP value required. This is the main reason why PG-case gains the highest CO_2 capture cost saving. Interestingly, in spite of a relatively higher HRP value required, PG-case still has the lower TMC area requirement than MEA-case, mainly caused by its higher heat flux per unit of TMC area. Due to the lower EXP value and higher POREV value, PG-case has a relatively higher CO_2 capture cost saving than MEA-case ($4.07/t-$CO_2$). Although PZ-case has the lowest EXP value as shown in Table 7, its CO_2 capture cost saving of $3.50/t-$CO_2$ is still lower than MEA- and PG-cases, which is mainly caused by its lower POREV value.

4. Conclusions

In this study, the transport membrane condenser (TMC) was set as the heat exchanger in the rich-split (RS) modified carbon capture process, in which the waste heat from the stripping gas was recovered by the bypassed cold rich solvent. The waste heat recovery performance was investigated and compared when the same TMC was used in MEA-, DEA-, PZ- and PG-based RS modification carbon capture processes. When taking MEA as an example, all the data on waste heat recovery performance falls within ±10% deviation through a 220-h continuous operation, showing the TMC has a good stability on the waste heat recovery performance in a long-term operation.

Parametric studies showed that when using a same TMC, PZ-case can achieve a highest waste heat recovery performance among all the four cases under the same operation conditions. The empirical correlations between the heat flux and mass flux during heat recovery were proposed for all the cases, which can provide an insight into the enhancement of heat recovery performance. The economic analysis on TMC-based RS modification carbon capture processes using different solvents was explored for clearly understanding the CO_2 capture cost savings in three different scenarios. In this scenario with a fixed TMC area, PZ-case gained a highest CO_2 capture cost saving ($6.40/t-$CO_2$), followed by PG-case ($4.98/t-

Table 7
Economic analysis of TMC-modified RS carbon capture processes with different absorbents at a fixed reduction ratio of reboiler duty.

Item	Value			
Case No.	MEA-case	DEA-case	PZ-case	PG-case
Regeneration heat requirement (GJ/t-CO_2)	~4.0 [49]	~3.0 [50]	~3.4 [27]	~4.3 [31]
Reboiler duty saving ratio	15%			
HRP value (kJ/kg-CO_2)	600	450	510	645
$V_{\bar{A}}$ ($Nm^3/(h \cdot m^2)$)	33.6	36.8	82.4	44.8
Solvent flow rate (kg/h)	37.4	30.0	93.6	53.9
Required membrane area (m^2)	55.7	50.8	22.7	41.8
Additional cost of auxiliaries (valves, pipelines and pumps) ($)	14,006			
Additional cost of construction ($)	7842	7399	4856	6585
Additional yearly depreciation cost of RS modification ($/year)	1882	1776	1165	1581
C_M ($/year)	4214	3843	1717	3163
Additional cost of maintenance ($/year)	2801			
C_P ($/year)	934.3	747.4	2335.7	1121.1
Additional operation cost ($/year)	9831	9167	8020	8666
EXP ($/t-$CO_2$)	0.97	0.91	0.79	0.86
POREV ($/t-$CO_2$)	5.04	3.78	4.29	5.42
CO_2 capture cost saving ($/t-$CO_2$)	4.07	2.87	3.50	4.56

CO_2), MEA-case ($3.76/t-$CO_2$) and DEA ($2.77/t-CO_2). In the scenario with a fixed waste heat recovery performance of 600 kJ/kg-CO_2, PZ- and PG-case obtained the same highest CO_2 capture cost saving of $4.22/t-$CO_2$. In the scenario with a fixed 15% reduction rate of reboiler duty, PG-case achieved the maximum CO_2 capture cost saving ($4.56/t-$CO_2$).

It should be noted that a high CO_2 capture cost saving will be achieved in the future for the TMC-modified RS carbon capture process when the advanced membrane with a low price and high mass transfer performance can be adopted. Furthermore, this TMC modification process can be further optimized via some complementary process modelling techniques like Aspen Plus software to minimize the costs related to the TMC modification, which will lead to a high CO_2 capture cost saving as well.

Credit author statement

All authors contributes to the preparation of the previous and revised manuscript, which can be seen as follows: Supervised by Shuiping Yan, Qiufang Cui has done all the experiments and data analysis of waste heat recovery performance. Te Tu has helped collect the data and completed the techno-economic evaluation part. Shuiping Yan has done the experimental design. Qiufang Cui has written the draft manuscript. Te Tu has performed the manuscript organization. Shuiping Yan and Long Ji have edited and checked the manuscript.

Declaration of competing interest

The authors declare that they have no known competing financial interests or personal relationships that could have appeared to influence the work reported in this paper.

Acknowledgements

The authors wish thank the financial supports from the National Key R&D Program of China (No. 2017YFB0603300), the National Natural Science Foundation of China (No. 51676080) and the Fundamental Research Funds for the Central Universities (No. 2662018PY046).

Nomenclature

A	Membrane area (m^2)
c	Averaged specific heat capacity of rich solvent (kJ/(kg K))
C_M	Membrane replacement cost ($/year)
C_P	Power consumption cost (liquid pump) ($/year)
DEA	Diethanolamine
EXP	Expenditure due to the additional investment and corresponding operation and maintenance costs ($/t-$CO_2$)
$h(T)$	Enthalpy at the temperature T (kJ/kg)
HRP	Heat recovery performance
I.D.	Inner dimension (mm)
J	Recovered water flux (kg/(m^2 h))
m	Mass flow rate, kg/h
MEA	Monoethanolamine
O&M	Operation and maintenance costs ($/t-$CO_2$)
O.D.	Outer dimension (mm)
P	Pressure (kPa)
PG	Potassium glycinate
POREV	Potential revenue due to steam saving ($/t-$CO_2$)
PZ	Piperazine
Q	CO_2 regeneration heat saving (kJ/kg-CO_2)
q	Heat recovery flux per m^2 of membrane area (MJ/(m^2 h))
RS	Rich split
T	Temperature (°C)
TMC	Transport membrane condenser
V	Volumetric flow rate (Nm^3/h or L/h)
$V_{\bar{A}}$	Stripping gas volumetric flow rate per unit of membrane area ($Nm^3/(h \cdot m^2)$)
W	Solvent concentration (wt.%)

Subscripts and superscripts

By	Bypassed solvent
in	Inlet
out	Outlet
sol	Solvent
Tot	Total
v	Water vapor
w	Water

Greek letter

α_{Tot}	CO_2 loading
γ	Molar ratio of water vapor to CO_2
η	Split fraction

ϕ The absolute humidity of water vapor saturated CO_2 at −2 °C

References

[1] Feron PHM, Cousins A, Gao S, Liu L, Wang J, Wang S, Niu H, Yu H, Li K, Cottrell A. Experimental performance assessment of a mono-ethanolamine-based post-combustion CO_2-capture at a coal-fired power station in China. Greenh Gases 2017;7:486–99.
[2] Kim H, Hwang SJ, Lee KS. Novel shortcut estimation method for regeneration energy of amine solvents in an absorption-based carbon capture process. Environ Sci Technol 2015;49:1478–85.
[3] Wang T, He H, Yu W, Sharif Z, Fang M. Process simulations of CO_2 desorption in the interaction between the novel direct steam stripping process and solvents. Energy Fuels 2017;31:4255–62.
[4] Zhao S, Feron PHM, Deng L, Favre E, Chabanon E, Yan S, Hou J, Chen V, Qi H. Status and progress of membrane contactors in post-combustion carbon capture: a state-of-the-art review of new developments. J Membr Sci 2016;511:180–206.
[5] Cousins A, Wardhaugh LT, Feron PHM. Preliminary analysis of process flow sheet modifications for energy efficient CO_2 capture from flue gases using chemical absorption. Chem Eng Res Des 2011;89:1237–51.
[6] Cousins A, Cottrell A, Lawson A, Huang S, Feron PHM. Model verification and evaluation of the rich-split process modification at an Australian-based post combustion CO_2 capture pilot plant. Greenh Gases 2012;2:329–45.
[7] Lin Y-J, Madan T, Rochelle GT. Regeneration with rich bypass of aqueous piperazine and monoethanolamine for CO_2 capture. Ind Eng Chem Res 2014;53:4067–74.
[8] Bao A, Wang D, Lin C-X. Nanoporous membrane tube condensing heat transfer enhancement study. Int J Heat Mass Tran 2015;84:456–62.
[9] Wang D, Bao A, Kunc W, Liss W. Coal power plant flue gas waste heat and water recovery. Appl Energy 2012;91:341–8.
[10] Wang T, Yue M, Qi H, Feron PHM, Zhao S. Transport membrane condenser for water and heat recovery from gaseous streams: performance evaluation. J Membr Sci 2015;484:10–7.
[11] Horikawa T, Do DD, Nicholson D. Capillary condensation of adsorbates in porous materials. Adv Colloid Interface Sci 2011;169:40–58.
[12] Uhlhorn RJR, Keizer K, Burggraaf AJ. Gas transport and separation with ceramic membranes. Part I. Multilayer diffusion and capillary condensation. J Membr Sci 1992;66:259–69.
[13] Xiao L, Yang M, Zhao S, Yuan W-Z, Huang S-M. Entropy generation analysis of heat and water recovery from flue gas by transport membrane condenser. Energy 2019;174:835–47.
[14] Yan S, Cui Q, Xu L, Tu T, He Q. Reducing CO_2 regeneration heat requirement through waste heat recovery from hot stripping gas using nanoporous ceramic membrane. Int J Greenh Gas Control 2019;82:269–80.
[15] Zhou Y, Chen H, Xie T, Wang B, An L. Effect of mass transfer on heat transfer of microporous ceramic membranes for water recovery. Int J Heat Mass Tran 2017;112:643–8.
[16] Chen H, Zhou Y, Cao S, Li X, Su X, An L, Gao D. Heat exchange and water recovery experiments of flue gas with using nanoporous ceramic membranes. Appl Therm Eng 2017;110:686–94.
[17] Chen H, Zhou Y, Su X, Cao S, Liu Y, Gao D, An L. Experimental study of water recovery from flue gas using hollow micro–nano porous ceramic composite membranes. J Ind Eng Chem 2018;57:349–55.
[18] Samaei SM, Gato-Trinidad S, Altaee A. The application of pressure-driven ceramic membrane technology for the treatment of industrial wastewaters – a review. Separ Purif Technol 2018;200:198–220.
[19] Hu HW, Tang GH, Niu D. Wettability modified nanoporous ceramic membrane for simultaneous residual heat and condensate recovery. Sci Rep 2016;6:27274–84.
[20] Kim JF, Park A, Kim S-J, Lee P, Cho Y, Park H, Nam S, Park Y. Harnessing clean water from power plant emissions using membrane condenser technology. ACS Sustainable Chem Eng 2018;6:6425–33.
[21] Li Z, Zhang H, Chen H. Application of transport membrane condenser for recovering water in a coal-fired power plant: a pilot study. J Clean Prod 2020;261:121229.
[22] Gao D, Li Z, Zhang H, Zhang J, Chen H, Fu H. Moisture recovery from gas-fired boiler exhaust using membrane module array. J Clean Prod 2019;231:1110–21.
[23] Yan S, Zhao S, Wardhaugh L, Feron PH. Innovative use of membrane contactor as condenser for heat recovery in carbon capture. Environ Sci Technol 2015;49:2532–40.
[24] Yan S, Cui Q, Tu T, Xu L, He Q, Feron PHM, Zhao S. Membrane heat exchanger for novel heat recovery in carbon capture. J Membr Sci 2019;577:60–8.
[25] Cui Q, Liu S, Xu L, Tu T, He Q, Yan S. Modification of rich-split carbon capture process using ceramic membrane for reducing the reboiler duty: effect of membrane arrangements. Separ Purif Technol 2020;235:116148–58.
[26] Xu L, Cui Q, Tu T, Liu S, Ji L, Yan S. Waste heat recovery from the stripped gas in carbon capture process by membrane technology: hydrophobic and hydrophilic organic membrane cases. Greenh Gases 2020;10:421–35.
[27] Rochelle GT, Wu Y, Chen E, Akinpelumi K, Fischer KB, Gao T, Liu C-T, Selinger JL. Pilot plant demonstration of piperazine with the advanced flash stripper. Int J Greenh Gas Control 2019;84:72–81.
[28] Bernhardsen IM, Knuutila HK. A review of potential amine solvents for CO_2 absorption process: absorption capacity, cyclic capacity and pKa. Int J Greenh Gas Control 2017;61:27–48.
[29] Bishnoi S, Rochelle GT. Absorption of carbon dioxide into aqueous piperazine: reaction kinetics, mass transfer and solubility. Chem Eng Sci 2000;55:5531–43.
[30] Chen J, Luo W, Li H. A review for research on thermodynamics and kinetics of carbon dioxide absorption with organic amines. J Chem Ind Eng (China)) 2014;65:12–21 [Chinese].
[31] Zhou XP. Experimentalstudy on the characteristics of amino acid salts and blended CO_2 absorbents [dissertation]. Hangzhou (Zhejiang): Zhejiang University; 2016 [Chinese].
[32] Caumon M-C, Sterpenich J, Randi A, Pironon J. Experimental mutual solubilities of CO_2 and H_2O in pure water and NaCl solutions. Energy Procedia 2017;114:4851–6.
[33] Ghidossi R, Carretier E, Veyret D, Dhaler D, Moulin P. Optimizing the compacity of ceramic membranes. J Membr Sci 2010;360:483–92.
[34] Hofs B, Ogier J, Vries D, Beerendonk EF, Cornelissen ER. Comparison of ceramic and polymeric membrane permeability and fouling using surface water. Separ Purif Technol 2011;79:365–74.
[35] Kilduff JE, Mattaraj S, Pieracci JP, Belfort G. Photochemical modification of poly(ether sulfone) and sulfonated poly(sulfone) nanofiltration membranes for control of fouling by natural organic matter. Desalination 2000;132:133–42.
[36] Weiland RH, Dingman JC, Cronin DB. Heat capacity of aqueous monoethanolamine, diethanolamine, n-methyldiethanolamine, and n-methyldiethanolamine-based blends with carbon dioxide. J Chem Eng Data 1997;42:1004–6.
[37] Chenlo F, Moreira R, Pereira G, Vázquez MJ, Santiago E. Viscosities of single-solute and binary-solute aqueous systems of monoethanolamine, diethanolamine, and 2-amino-2-methyl-1-propanol. J Chem Eng Data 2001;46:276–80.
[38] Khayet M, Godino MP, Mengual JI. Thermal boundary layers in sweeping gas membrane distillation processes. AIChE J 2002;48:1488–97.
[39] Zhao S, Wardhaugh L, Zhang J, Feron PHM. Condensation, re-evaporation and associated heat transfer in membrane evaporation and sweeping gas membrane distillation. J Membr Sci 2015;475:445–54.
[40] Rabensteiner M, Kinger G, Koller M, Hochenauer C. PCC pilot plant studies with aqueous potassium glycinate. Int J Greenh Gas Control 2015;42:562–70.
[41] Yue M, Zhao S, Feron PHM, Qi H. Multichannel tubular ceramic membrane for water and heat recovery from waste gas streams. Ind Eng Chem Res 2016;55:2615–22.
[42] Tu T, Liu S, Cui Q, Xu L, Ji L, Yan S. Techno-economic assessment of waste heat recovery enhancement using multi-channel ceramic membrane in carbon capture process. Chem Eng J 2020;400:125677.
[43] Soleimanikutanaei S, Lin C-X, Wang D. Numerical modeling and analysis of transport membrane condensers for waste heat and water recovery from flue gas. Int J Therm Sci 2019;136:96–106.
[44] Zhao S, Yan S, Wang DK, Wei Y, Qi H, Wu T, Feron PHM. Simultaneous heat and water recovery from flue gas by membrane condensation: experimental investigation. Appl Therm Eng 2017;113:843–50.
[45] Le Moullec Y, Kanniche M. Screening of flowsheet modifications for an efficient monoethanolamine (MEA) based post-combustion CO_2 capture. Int J Greenh Gas Control 2011;5:727–40.
[46] Yan S, Fang M, Zhang W, Zhong W, Luo Z, Cen K. Comparative analysis of CO_2 separation from flue gas by membrane gas absorption technology and chemical absorption technology in China. Energy Convers Manag 2008;49:3188–97.
[47] Zhang X, Wu J, Li Z, Chen Y. A hybrid flue gas heat recovery system based on vapor compression refrigeration and liquid desiccant dehumidification. Energy Convers Manag 2019;195:157–66.
[48] Wu J. Life cycle environment assessment of post cmbustion carbon dioxide capture system [dissertation]. Hangzhou (Zhejiang): Zhejiang University; 2019 [Chinese].
[49] Li K, Leigh W, Feron P, Yu H, Tade M. Systematic study of aqueous monoethanolamine (MEA)-based CO_2 capture process: techno-economic assessment of the MEA process and its improvements. Appl Energy 2016;165:648–59.
[50] Rodríguez N, Mussati S, Scenna N. Optimization of post-combustion CO_2 process using DEA–MDEA mixtures. Chem Eng Res Des 2011;89:1763–73.